




A MECHANO-BIOLOGICAL STUDY COMPARING EXTERNAL FIXATION USING MONOCORTICAL AND BICORTICAL PINS IN TIBIAL DIAPHYSEAL FRACTURE MODELS: A FINITE ELEMENT ANALYSIS

TARGOL BAYAT 

*Department of Mechanical and Aerospace Engineering
Polytechnic University of Turin, Turin, Italy
targol.bayat@studenti.polito.it*

YOUSOF MOHANDÉS * and MOHAMMAD TAHAMI †

*Bone and Joint Disease Research Center
Shiraz University of Medical Sciences, Shiraz, Iran
*yousofmohandes@gmail.com
†mohammad.tahami@yahoo.com*

MASOUD TAHANI ‡

*Department of Mechanical Engineering
Ferdowsi University of Mashhad, Mashhad, Iran
mtahani@um.ac.ir*

Received 3 January 2023

Revised 10 June 2023

Accepted 28 September 2023

Published 20 November 2023

Extramedullary devices are used extensively to stabilize fractures in long bones. The type of pin–bone anchorage is a determining factor in fixation properties, which differ between mono-cortical and bi-cortical stabilizations. This computational study compares the effects of mono-cortical and bi-cortical pins of a unilateral uniplanar external fixator on the construct stiffness, the early phase of bone healing, and pin loosening. Eight finite element models were established for a simple transverse tibia fracture, treated with a unilateral uniplanar external fixator with surgical variations in the pin–bone anchorage. Each model was subjected to a partial body weight, and axial stiffness was calculated. A deviatoric strain-based mechano-regulation algorithm was applied, and tissue differentiation in the callus was predicted. Finally, a strain-based failure criterion was employed to assess the risk of pin loosening. The axial stiffnesses of bi-cortical structures were slightly larger than the results of the mono-cortical sets. Regardless of the number of pins, bi-cortical systems produce a more uniform distribution of differentiated tissue than the corresponding mono-cortical constructs. Finally, both mono-cortical and bi-cortical groups held the critical strains of the pin–bone interface within the acceptable ranges and provided a protected construct against the risk of pin loosening. Based on the findings of this study, mono-cortical pins could be considered potential alternatives to

‡Corresponding author.

bi-cortical fixations at the early stage of healing. Nevertheless, successful management of diaphyseal fracture through mono-cortical fixation needs to be assessed in further studies over the full period of healing.

Keywords: Tibial diaphyseal fracture; unilateral-uniplanar external fixator; mechano-biology of bone healing; mono-cortical pins; bi-cortical pins; pin loosening.

1. Introduction

Tibial fracture accounts for a significant proportion of long bone fractures, a high percentage of which occurs as open fractures.^{1,2} Surgical interventions for fixating these fractures should overcome many challenges, including the risk of implant failure, infection, instability, bone malalignment, impaired healing, and re-fracture after implant removal.³ External fixation is among the common osteosynthesis modalities employed for anatomic alignment and stabilization of open or severe closed fractures.⁴⁻⁶ Since the external fixators are placed outside the extremity, the fracture could be immobilized without the need for open reduction.^{7,8} The incision made during the surgery is limited, and the blood supply to the fracture site is less disturbed.⁹ In this circumstance, external fixation is a suitable treatment for patients who cannot endure an open procedure or suffer from hemodynamically unstable conditions.²

The most common external fixator for treating long bone fractures is the unilateral-uniplanar frame, which includes a side connecting rod with bi-cortical Schanz pins and clamps.^{8,10} Despite its extensive clinical usage, bi-cortical fixation suffers from several devastating complications. Bi-cortical Schanz pins penetrate the near and far cortices and pass through the medullary canal, thus causing damage to the vascular network.⁴ In bi-cortical fixation, drilling the second cortex by self-drilling pins may destroy the threaded entrance formerly prepared at the first cortex.¹¹ Moreover, bi-cortical fixations increase the risk of thermal damage to the surrounding tissue and the bone itself.¹² What is more, bi-cortical pins make secondary surgeries problematic for cases with a two-step surgery scenario. In late cases, a primary external fixation is followed by an internal surgery via plating or intramedullary nailing as the definitive treatment. As for the secondary surgery via nailing, bi-cortical pins must be pulled back to let the nail pass through the medullary canal, which increases pin loosening and infection risks.⁸ Therefore, there has been an emerging trend in recent orthopedic biomechanics literature toward using mono-cortical constructs as alternatives to bi-cortical ones.^{8,12-14}

Previous studies have shown mono-cortical fixation systems performed comparably to the bi-cortical systems, in terms of structural strength, static stability, and dynamic durability.^{4,8,13} However, quantitative mechano-biological aspects of external fixation under different pin-bone anchorages have not been investigated yet. The objective of this study is to assess the axial stiffness, risk of pin loosening, and healing outcome of unilateral-uniplanar external fixator of various pin arrangements fixed by mono-cortical or bi-cortical pins in the treatment of the tibial diaphyseal

fracture. To this end, by employing finite element-based computational modeling, a mechano-regulatory algorithm of bone healing and a strain-based failure criterion were adopted to predict tissue differentiation and pin loosening at the early phase of the repairing process, respectively.

2. Materials and Methods

Two groups of FE models were generated to compare healing outcomes and pull-out strength in the early postoperative phase: mono-cortical and bi-cortical. Each group comprised four models fixed by 2, 4, 6, and 8 pins (Fig. 1). Although external

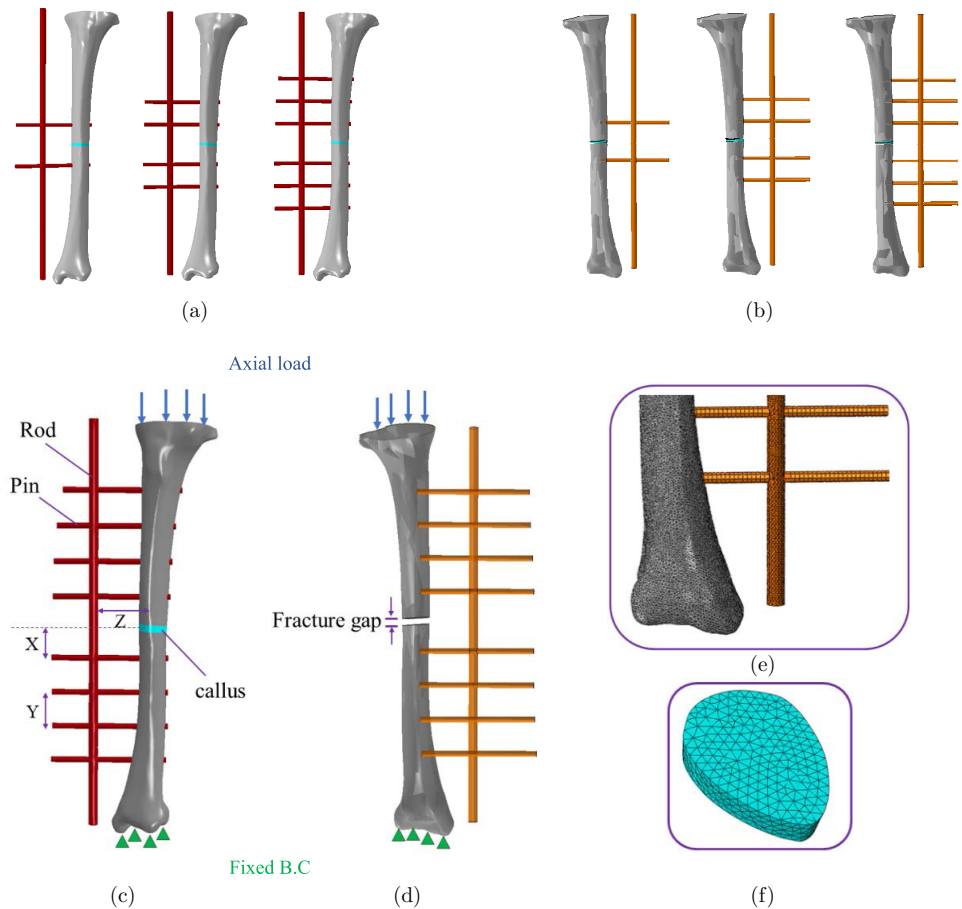


Fig. 1. (a) The bi-cortical group includes 2BiC, 4BiC, and 6BiC; (b) the mono-cortical group includes 2MoC, 4MoC, and 6MoC; (c), (d) illustrate vertical downward load acted on the proximal end, and restrained boundary condition at the distal end of a sample construct with eight pins: 8BiC and 8MoC. Distance of the nearest pin to the fracture site, the distance between consecutive pins, and rod elevation were labeled as X , Y , and Z , respectively; (e) a zoomed view of finite element mesh generated on the tibia, rod, and pin; and (f) discretized model of central callus composed of endosteal and intercortical regions.

configuration with only one pin per segment is not a clinically viable option, it was considered to get a bigger picture of the trends. Throughout this paper, two terms, n MoC and n BiC, were defined for brevity, where n represents the number of pins, MoC stands for mono-cortical, and BiC means bi-cortical. The different numbers of the pin were intentionally examined in this study to consider their effect on the stiffness, pin loosening, and healing responses of MoC/BiC groups.

A series of 681 computed tomography (CT) images of a 27-year-old healthy woman's left tibia was procured, processed, and converted into point cloud (txt file format) using Mimics Innovation Suite software (V21, Materialise, Belgium). The point cloud file was transferred into the computer-aided design software of Catia (V5. R21, Dassault Systèmes, France) to build a three-dimensional solid model of the intact tibia. Subsequently, a simple transverse fracture with a gap size of 3 mm was embedded in the mid-diaphyseal region of the tibia model according to AO/OTA classification (42-A3). The geometric model of the external fixator was established using specifications given in the implant manufacturer catalog (DePuy Synthes Co., Ltd, New Brunswick, CA, USA). Accordingly, pins with 5 mm diameter and 100 mm length and the rod with 8 mm diameter and 350 mm length were designed, assembled, and virtually installed on the anteromedial side of the tibia model. The pin threads were neglected for simplification, but their mechanical and biomechanical effects were considered in the boundary constraints.¹⁵ Pins in the MoC group penetrated just into the first bone cortex near the rod, while in the BiC group, they inserted up to the second cortex, far from the rod. The transverse distance of 50 mm was set between the tibial anatomical axis and the longitudinal axis of the rod. The distance between the first pin and the fracture site and between two consecutive pins was 25 mm and 30 mm, respectively. Furthermore, the number of pins was kept identical for proximal and distal fragments of the broken bone.

Since the external periosteal callus does not form at the early stage of healing,¹⁶ only the central callus was simulated in this study, which represented endosteal and intercortical regions. The geometric models were then imported into Abaqus (V6.14-5, Dassault Systèmes, France) to generate the volumetric mesh. The mesh verification test was carried out using the strain and stiffness criteria, and the optimum mesh size for the callus converged at 1 mm, while bone, pin, and rod converged at 2 mm. Table 1 summarizes mesh characteristics for each part in the FE model.

After that, the volumetric mesh was imported into Mimics again to assign the material properties to each bone element. A Hounsfield Unit of 700 was employed to segment cortical and cancellous bone tissue contours in CT images.¹⁹ The pin and rod were considered to be made of stainless steel. All materials were homogeneous and isotropic with linear elastic mechanical behavior. Material properties of the bone and implant components are given in Table 1.

The remaining FE analysis pre-processing phases were carried out in Abaqus. The fully bonding tie constraints were implemented for describing the interactions between all surfaces in contact, i.e., pin-rod, pin-bone, and callus-bone interfaces.

Table 1. Mesh characteristics and material properties in the FE model.

Part	Young's modulus (MPa)	Poisson's ratio	Element type
Cortical bone	17,000 ^a	0.3 ^a	C3D10 ^c
Cancellous bone	700 ^a	0.2 ^a	C3D10
Rod	200,000	0.3	C3D4 ^d
Pin	200,000	0.3	C3D8 ^e
Callus	1 (refer Table 3) ^b	0.167 (refer Table 3) ^b	C3D10

^aRefer Ref. 17.^bRefer Ref. 18.^cTen-node quadratic tetrahedral.^dFour-node linear tetrahedral.^eEight-node linear brick.

Applying the tie constraint is an adequate analytical alternative to compensate for neglected threads and clamps' mechanical and biomechanical effects. According to the AO guideline, a vertical downward load case that equals 20% of body weight for a 75 kg patient was applied as a uniform pressure on the proximal end of the tibia to simulate partial weight-bearing during early post-surgery rehabilitation practice.²⁰ All degrees of freedom were constrained at the distal end of the tibia to prevent rigid body motion.

Initially, the entire fracture gap was filled with granulation tissue. The axial stiffness of each case was determined as the ratio of axial load (i.e., the partial body weight) to interfragmentary axial displacement at the fracture site. To monitor the early differentiation of granulation tissue, the deviatoric strain-based mechano-regulation algorithm was used. The algorithm has been indirectly validated for predicting the course of normal fracture healing.²¹ Accordingly, the deviatoric strain (ε_d) acts as the mechanical stimulus inside the callus and characterizes the new tissue phenotype (Table 2),²¹ and defined as follows:

$$\varepsilon_d = \frac{2}{3} \sqrt{(\varepsilon_1 - \varepsilon_2)^2 + (\varepsilon_1 - \varepsilon_3)^2 + (\varepsilon_2 - \varepsilon_3)^2}, \quad (1)$$

where ε_1 , ε_2 , and ε_3 indicate the three principal strains at each callus element. A custom Python script was developed to calculate the element-wise deviatoric strain and subsequently attribute a new tissue type to each callus element.

Table 2. Properties and tissue phenotypes of callus elements are classified according to the deviatoric strain theory.²¹

Deviatoric strain % (ε_d)	Tissue type	Young's modulus (MPa)	Poisson's ratio
$\varepsilon_d = 100$	Granulation tissue	1	0.167
$5 \leq \varepsilon_d < 100$	Fibrous	1-5	0.167
$2.5 \leq \varepsilon_d < 5$	Cartilage	5-500	0.167
$0.05 \leq \varepsilon_d < 2.5$	Immature bone	500-1000	0.325
$0.041 \leq \varepsilon_d < 0.05$	Intermediate bone	1000-2000	0.325
$0.005 \leq \varepsilon_d < 0.041$	Mature bone	2000-6000	0.325
$\varepsilon_d < 0.005$	Resorption	—	—

Finally, a strain-based failure criterion was adopted to check the potential for bone yielding at the pin–bone interface and the initiation of pin loosening under partial body weight. Accordingly, the tensile and compressive yield strains were assumed to be 0.5% and -0.7% , respectively.²²

3. Results

3.1. Axial stiffness

The axial stiffness of the bone-external fixator construct for BiC and MoC fixation groups is demonstrated in Fig. 2 for different numbers of pins ($n = \text{constant}$). The axial stiffness in the BiC group is slightly higher than that attained with the equivalent model in the MoC fixation. The mono-cortical external fixator reached the lowest axial rigidity using two pins ($n = 2$). Furthermore, it was found that the axial stiffness increased with the number of pins considerably when moving from $n = 2$ to $n = 4$ pins.

3.2. The average Young’s modulus (E_{avg})

The element-wise Young’s moduli resulted at the initial stage of healing averaged over the callus domain in different FE models are shown in Fig. 3. E_{avg} in the BiC group is higher than the MoC group for each n . For both BiC and MoC groups investigated, increasing the number of pins caused E_{avg} to rise in the callus. The highest E_{avg} was found in the 8BiC configuration, while the lowest E_{avg} was attributed to the 2MoC configuration.

3.3. The pattern of tissue differentiation

During the early stages of bone repair, healing domains in all numerical model variations were turned into tissue with Young’s moduli between 1 Mpa and 5 MPa,

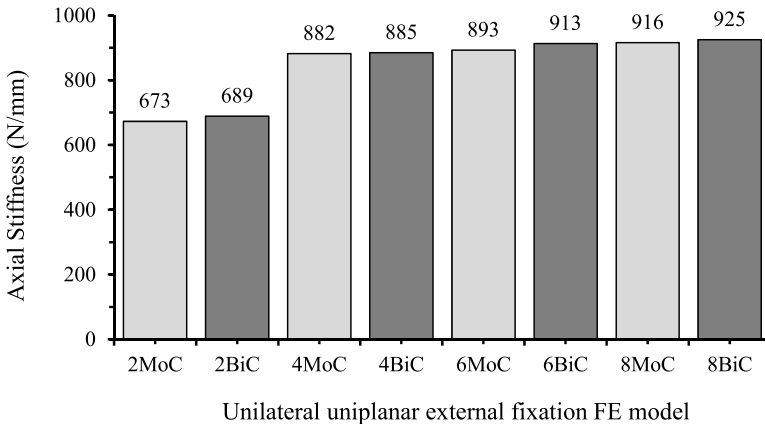


Fig. 2. The overall axial stiffness for eight FE models in BiC and MoC groups.

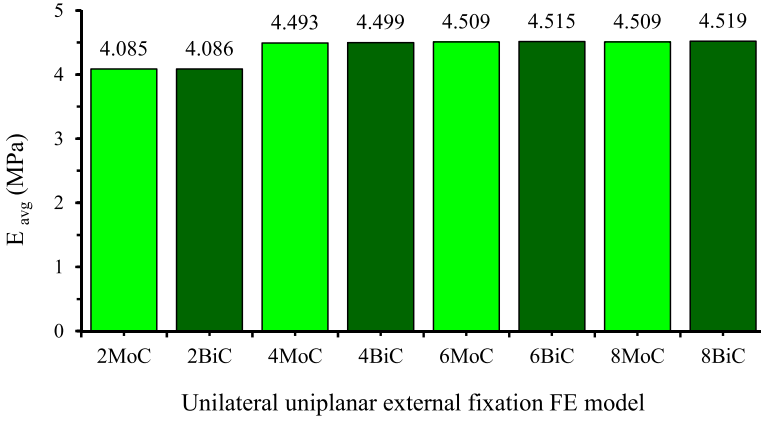


Fig. 3. The average Young’s modulus of callus elements in eight FE models in BiC and MoC groups.

corresponding to the range of fibrous tissue phenotype (Fig. 4). For all the configurations investigated, Fig. 4 discloses that the highest and lowest Young’s modulus regions were produced at the near and far cortex, respectively.

The deformed shape of the bone-fixator structure due to axial force with a scaling factor of 11 is shown in Fig. 5. For all specimens, the displacement of the fracture site toward the far cortex is greater than that of the near cortex, which affects the callus tissue differentiation.

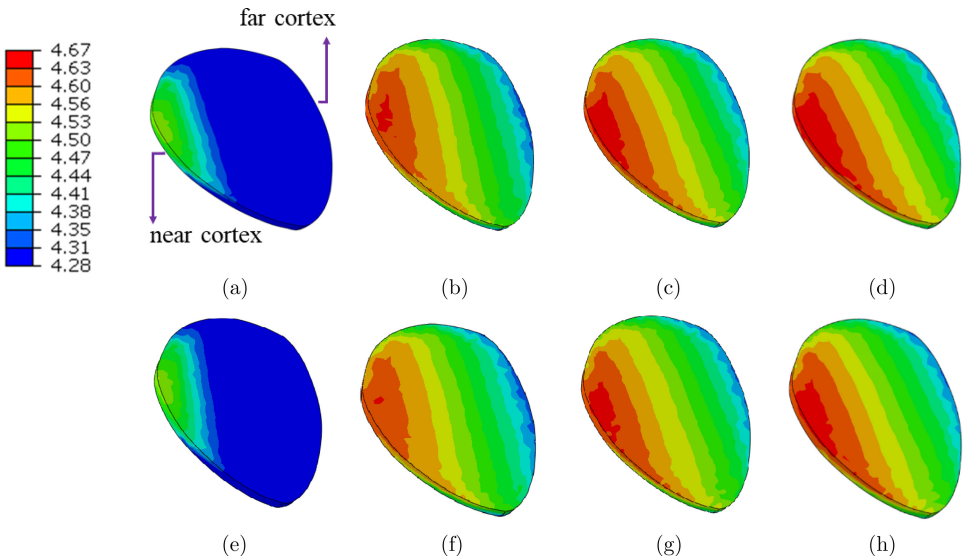


Fig. 4. Young’s modulus (MPa) contour plot in callus for fixation models: (a) 2BiC, (b) 4BiC, (c) 6BiC, (d) 8BiC, (e) 2MoC, (f) 4MoC, (g) 6MoC, and (h) 8MoC.

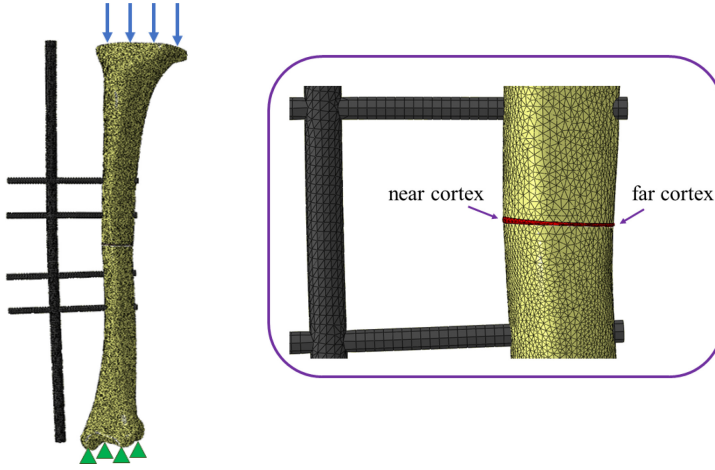


Fig. 5. Near and far cortex callus elements realize different displacements due to the bending induced in the fractured bone.

3.4. The uniformity of tissue differentiation

The uniformity in tissue differentiation was evaluated by calculating the difference between the maximum (E_{\max}) and minimum (E_{\min}) Young's moduli at the repair tissue and is reported as E_{dif} in the last row of Table 3. A lower value of E_{dif} indicates more uniform tissue differentiation. The BiC fixation resulted in a slightly more uniform differentiation than the MoC fixation for each n . For $n = 4, 6,$ and 8 pins, E_{dif} was below 0.4 MPa across all tested groups. In contrast, at $n = 2$, E_{dif} exceeded 1 MPa.

3.5. The risk of pin loosening

Figure 6 shows the distributions of maximum principal strain (top row) and minimum principal strain (bottom row) in the bone segments. The highest principal strains arise at the pin insertion sites near the fracture zone, as identified by a 4-point star.

Figure 7 shows that under the axial load of 20% of the body weight, which resembled the partial body weight in the initial days after surgery, neither bi-cortical

Table 3. Difference between the minimum and maximum Young's modulus among the callus elements.

Young's modulus (E)	2BiC	2MoC	4BiC	4MoC	6BiC	6MoC	8BiC	8MoC
E_{\min} (MPa)	3.524	3.519	4.271	4.264	4.293	4.286	4.297	4.283
E_{\max} (MPa)	4.527	4.53	4.669	4.663	4.667	4.661	4.666	4.657
E_{dif} (MPa)	1.003	1.011	0.398	0.399	0.374	0.375	0.369	0.374

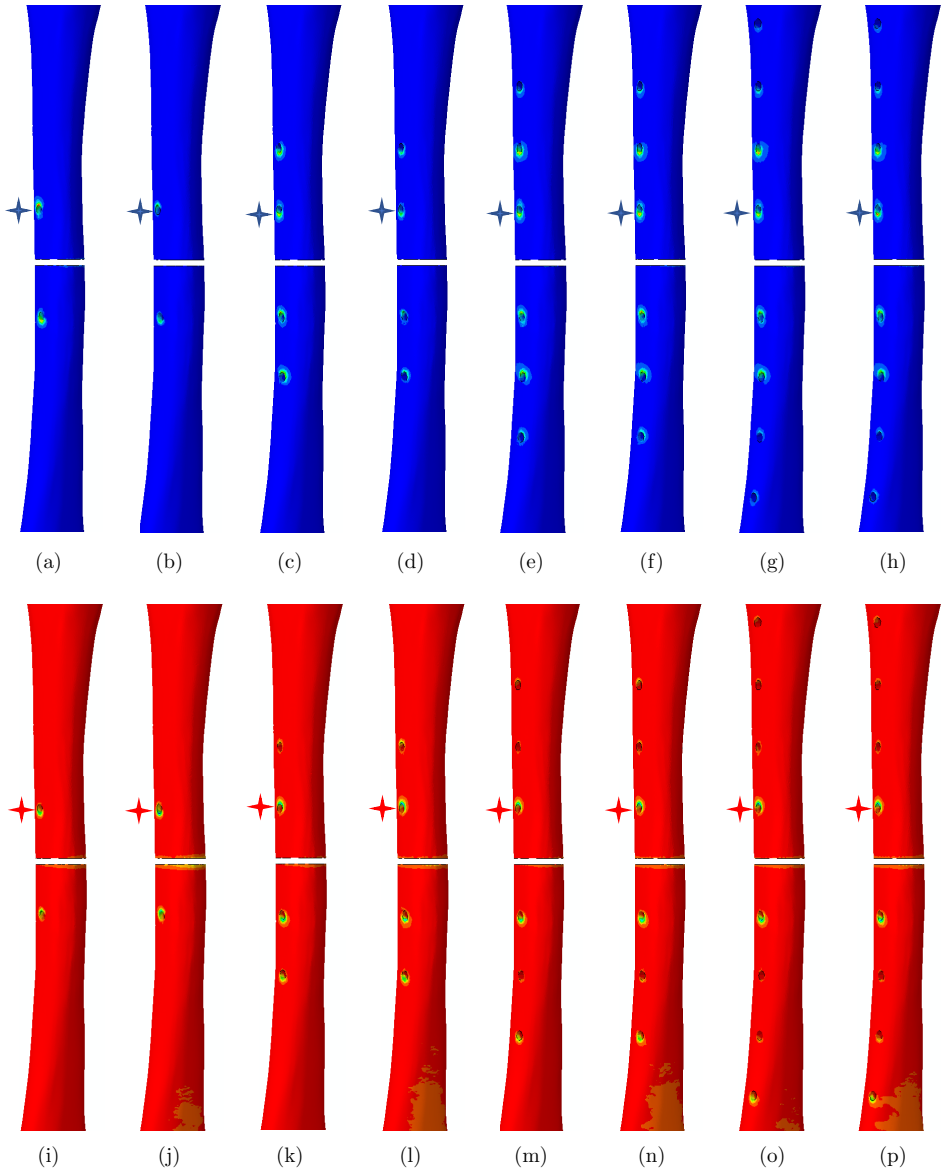
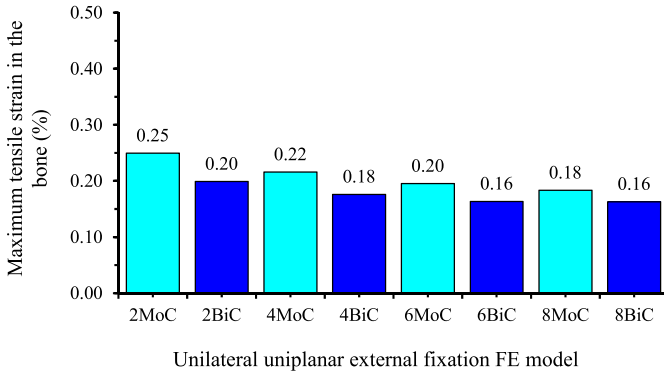
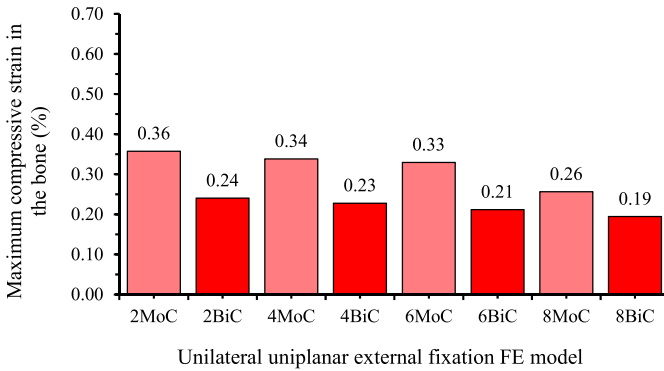


Fig. 6. The top row shows the maximum principal strain distribution in the bone for (a) 2MoC, (b) 2BiC, (c) 4MoC, (d) 4BiC, (e) 6MoC, (f) 6BiC, (g) 8MoC, and (h) 8BiC. The bottom row shows the minimum principal strain distribution in the bone for (i) 2MoC, (j) 2BiC, (k) 4MoC, (l) 4BiC, (m) 6MoC, (n) 6BiC, (o) 8MoC, and (p) 8BiC. The 4-point star indicates the critical location.

nor mono-cortical groups reached the maximum allowable tensile or compressive strains at the pin–bone interface. Meanwhile, bi-cortical cases show lower interfacial strains than mono-cortical cases. For both BiC and MoC groups, the critical strain decreased as the number of pins was increased.



(a)



(b)

Fig. 7. The maximum strain at the pin–bone interface in the initial days after surgery: (a) tensile and (b) compressive.

4. Discussion

Comminuted fractures associated with soft tissue injury and high contamination should be fixed immediately to minimize post-traumatic complications.²³ In these cases, external fixators are used as temporary or definitive treatment.^{24,25} This numerical study aimed to assess the biomechanical and mechano-biological distinction between the bi-cortical and mono-cortical groups of varying pin configurations to treat diaphyseal tibial fractures using unilateral-uniplanar external fixators.

This study shows that the BiC fixations are more conducive to higher axial stiffness than the MoC designs (Fig. 2). It stands to reason that the pins in BiC fixation are anchored at two cortices, and bone fragments are displaced less than the MoC group under the applied load. The finding for the relation between the anchored length of the pin and the construct stiffness is consistent with the current literature. Varady *et al.*⁸ performed a clinical test on the porcine tibia fixed by an external fixator and came to the same conclusion. Ochman *et al.*²⁶ used locking and

nonlocking plates to treat metacarpal fractures in domestic pigs and showed that the axial stiffness provided by mono-cortical screws is smaller than bi-cortical types. As well, the results observed by Bonner *et al.*²⁷ in treating the distal tibial extra-articular fracture were similar to those found here. Of note, the axial stiffness obtained for the MoC system was slightly smaller than the BiC, but both are in the same range (Fig. 2). This result correlates well with that seen in the *in vitro* experiment by Mladenovic *et al.*⁴ who found that external fixators mounted by uni-cortical and Schanz pins almost exhibit the same stability in the mediolateral direction. The same conclusion was also reported in studies of other extramedullary devices that showed no remarkable difference in construct stiffness comparing the use of bi-cortical and mono-cortical screws.^{28,29} Although adding pins makes the construct stiffer, more than four pins did not substantially improve the stiffness (Fig. 2). Even though there is always a tendency to employ more pins to create a more stable construct, it should be kept in mind that increasing the number of pins elevates the risk of infection around the pin insertion area.⁸

Figure 3 indicates that the mean Young's modulus of the tissue obtained throughout the callus increases by adding pins and enhancing the stiffness of the construct. This effect is rooted in the coherence between the construct stiffness and the pathway of bone healing applied by the mechano-regulation theory used in this study.³⁰ Accordingly, the negligible difference between the axial stiffness of MoC and BiC groups (Fig. 2) is projected onto the mean Young's modulus of corresponding differentiated tissue. The most noticeable difference was found between the fixators with 2 and 4 pins, which can be explained by the axial stiffness reported for these two models (see Fig. 2).

Fibrous tissue produced at the fracture gap in all models indicated that granulation tissue elements experienced high magnitudes of mechanical stimuli at the initial stage of healing (Fig. 4). This result is confirmed by the findings of other studies, which showed that mechanical stimulus is higher at the central callus, and fibrocartilage tissue is expected to emerge at the early stage of healing.³⁰⁻³² In addition, Fig. 4 shows that for a similar number of pins, the distribution of Young's modulus throughout the callus is accordant in both MoC and BiC cases, given the identical mechanical stiffness provided by both fixation systems.

Although the entire construct is under an axial downward load, an asymmetric configuration and stiffness mismatch between implant and bone induce bending at the fracture site (Fig. 5). In this circumstance, the neutral axis is moved outside the bone section, close to a component with higher stiffness, i.e., the external fixator. Because of this factor, callus elements far from the neutral axis tend to be displaced higher than near-cortex elements close to the neutral axis (Fig. 5). Based on the mechano-regulation algorithm of bone healing employed in this study, the difference in axial displacements leads to regions with higher and lower Young's modulus at near and far cortices, respectively (Fig. 4). The findings of this study correspond to those of Bottlang *et al.*,³³ who conducted a histological evaluation of fracture healing

in a sheep tibia and found that minimal gap motion at the near cortex suppresses fibro-cartilage callus formation.

The results of tissue regeneration comparing different pin configurations demonstrate that at least four pins are required to achieve a uniform differentiation and an even distribution of tissue phenotypes across the callus (Table 3). Besides, it can be observed that changing the MoC to BiC fixation did not substantially improve the uniformity of biological response throughout the callus.

The location of maximum strain in the bone indicates that the loosening of pin contact with the surrounding bone mostly initiates from the entrance holes near the fracture site (Fig. 6). Our finding concerning the critical pin location is consistent with those of previous studies, which found that the pin–bone interface at the entrance site in the vicinity of the first fastener demonstrates the most proximity to yielding.^{22,34} Nonetheless, Figs. 7(a) and 7(b) show that during the first days after the insertion of pins, the bone strain around the pins do not go beyond the yield level, and subsequent pin loosening for either group BiC or MoC would not be a matter of concern. However, the smaller interfacial strain in bi-cortical groups indicates that their holding power in compact bone persists longer than in mono-cortical pins. Furthermore, as shown in Figs. 7(a) and 7(b), increasing the number of pins reduces the critical strain at the pin–bone interface due to the larger contact area. This can decrease the extent of localized bone yielding and the risk of subsequent pin loosening. Our finding confirms the results of previous studies, in which the volume of yielded bone and fixation instability were substantially reduced by employing extra pins.^{22,35}

The present computational research incorporated some assumptions and limitations that should be considered when interpreting the results. First, the models did not realize the pins' threads but assumed smooth surfaces tied to the bone tissue at pin–bone interfaces. Considering the fair corroboration that the FE model showed with previous research, this simplifying assumption was inappreciable. Therefore, it cannot be regarded as a significant source of error in the stiffness determination and mechanobiological part of this study. Nevertheless, the local effects of pin threads on the strain distribution across the bone cortices await further studies. Second, this study utilized the FE bone model of a healthy adult tibia, which exhibited a dense cortical thickness and did not suffer from osteoporosis. However, the complication of pin loosening depends on the quality of pin–bone interaction and could be exacerbated in patients with skeletal disorders, where the risk of cortical bone thinning is escalated.³⁶ Therefore, comparing the BiC and MoC fixations in pin loosening requires a deeper consideration of bone quality. The third parameter that can influence the analyses of this study was the simple transverse fracture geometry with perfectly flat surfaces and a gap size of 3 mm. A broader study that considers the fracture severity and complexity, e.g., oblique, butterfly, and comminuted fractures with irregular shapes and various gap sizes, could increase the robustness of the FE models and the accuracy of the predicted healing. Fourth, healing simulations were limited to the immediate phase, in which the granulation tissue presents at the

fracture gap. According to Nourisa and Rouhi,³⁷ we concluded that this limitation does not invalidate the overall reliability of the current results. They showed that the predicted tissue phenotype in the early bone healing stage correlates with the ultimate healing outcome. Nevertheless, extending the investigations to the entire course of healing and implying periosteal callus formation may likely yield a more rigorous comparison between BiC and MoC fixations. Finally, this study was limited to monitoring the tissue differentiation and failure of the pin–bone interface under the axial downward load of 20% body weight, which was applied as a uniform pressure. However, it is known that the partial body weight is transmitted to the tibia through the knee joint and is shared between medial and lateral condyles by 60% and 40%, respectively. Evaluating the strength and stability of the mono- and bi-cortical constructs subjected to higher loads and various loading scenarios applied at the actual locations may contribute to more accurate results.

5. Conclusion

The results of this study at the initial stage of healing indicated that MoC fixation is almost equivalent to BiC fixation in treating transverse tibial diaphyseal fractures under the unilateral-uniplanar external fixator. Furthermore, the absence of bone yielding and subsequent pin loosening in the MoC cases recommended them as stable fracture fixations in the immediate postoperative days. It appears to be a promising alternative to shift toward using MoC pins in the external fixators to discard the potential drawbacks of BiC fixations, e.g., deep infection, damage to surrounding tissues, and high amount of heat by passing through the bone cortices. Nonetheless, to transfer the findings of this study to a clinical arena, further examinations should be made for BiC versus MoC constructs based on other aspects of safe and satisfactory fixation, which were not addressed here.

Author Contributions

Conceptualization, Y. Mohandes; Data curation, T. Bayat; Formal analysis, T. Bayat; Investigation, M. Tahami; Methodology, Y. Mohandes; Project administration, M. Tahani; Validation, T. Bayat; Visualization, T. Bayat; Writing original draft, T. Bayat; Writing review and editing, Y. Mohandes.

Conflicts of Interest

There are no conflicts to declare.


Acknowledgments


We wish to show our gratitude to Dr. Alireza Shakibafard, TABA Medical diagnostic imaging center, for sharing bone CT images with us.


Funding


This research did not receive any specific grant from funding agencies in the public, commercial, or not-for-profit sectors.

ORCID

Targol Bayat  <https://orcid.org/0000-0003-4244-3718>

Yousof Mohandes  <https://orcid.org/0000-0002-6528-9090>

Mohammad Tahami  <https://orcid.org/0000-0002-3722-8426>

Masoud Tahani  <https://orcid.org/0000-0001-6174-2241>

References

1. Elniel AR, Giannoudis PV, Open fractures of the lower extremity: Current management and clinical outcomes, *EFORT Open Rev* **3**:316–325, 2018.
2. Hadeed A, Werntz RL, Varacallo M, External fixation principles and overview, in StatPearls Treasure Island: StatPearls Publishing, 2019.
3. Meleppuram JJ, Ibrahim S, Experience in fixation of infected non-union tibia by Ilizarov technique—a retrospective study of 42 cases, *Rev Bras* **52**:670–675, 2017.
4. Mladenovic D, Mitkovic M, Micic I, Karalejic S, Biomechanical tests and clinical application of unicortical pin by the external fixator system, *Biotechnol Biotec Eq* **17**:136–142, 2003.
5. Zhou Y, Wang Y, Liu L, Zhou Z, Cao X, Locking compression plate as an external fixator in the treatment of closed distal tibial fractures, *Int Orthop* **39**:2227–2237, 2015.
6. Koettstorfer J, Hofbauer M, Wozasek G, Successful limb salvage using the two-staged technique with internal fixation after osteodistraction in an effort to treat large segmental bone defects in the lower extremity, *Arch Orthop Traum Su* **132**:1399–1405, 2012.
7. Goh J, Thambyah A, Ghani AN, Bose K, Evaluation of a simple and low-cost external fixator, *Injury* **28**:29–34, 1997.
8. Varady PA, Greinwald M, Augat P, Biomechanical comparison of a novel monocortical and two common bicortical external fixation systems regarding rigidity and dynamic stability, *Biomed Eng-Biomed Tech* **63**:665–672, 2018.
9. Ang B, Chen J, Yew A, Chua S, Chou S, Chia S, Koh J, Howe T, Externalised locking compression plate as an alternative to the unilateral external fixator: A biomechanical comparative study of axial and torsional stiffness, *Bone Joint Res* **6**:216–223, 2017.
10. Roseiro LM, Neto MA, Amaro A, Leal RP, Samarra MC, External fixator configurations in tibia fractures: 1D optimization and 3D analysis comparison, *Comput Methods Prog Bio* **113**:360–370, 2014.
11. Arango D, Tiedeken N, Clippinger B, Samuel SP, Saldanha V, Shaffer G, Biomechanical analysis of four external fixation pin insertion techniques, *Orthop Rev* **9**:7067, 2017.
12. Greinwald M, Varady PA, Augat P, Unicortical self-drilling external fixator pins reduce thermal effects during pin insertion, *Eur J Trauma Emerg Surg* **44**:939–946, 2018.
13. Park K-H, Park H-W, Oh C-W, Lee J-H, Kim J-W, Oh J-K, Park I-H, Ha S-S, Conventional bicortical pin substitution with a novel unicortical pin in external fixation: A biomechanical study, *Injury* **52**:1673–1678, 2021.
14. Bliven EK, Greinwald M, Hackl S, Augat P, External fixation of the lower extremities: Biomechanical perspective and recent innovations, *Injury* **50**:S10–S17, 2019.

15. Nourisa J, Rouhi G, Biomechanical evaluation of intramedullary nail and bone plate for the fixation of distal metaphyseal fractures, *J Mech Behav Biomed* **56**:34–44, 2016.
16. Eastaugh-Waring S, Joslin C, Hardy J, Cunningham J, Quantification of fracture healing from radiographs using the maximum callus index, *Clin Orthop Relat Res* **467**:1986–1991, 2009.
17. Duda GN, Mandruzzato F, Heller M, Goldhahn J, Moser R, Hehli M, Claes L, Haas NP, Mechanical boundary conditions of fracture healing: borderline indications in the treatment of unreamed tibial nailing, *J Biomech* **34**:639–650, 2001.
18. Isaksson H, Van Donkelaar CC, Ito K, Sensitivity of tissue differentiation and bone healing predictions to tissue properties, *J Biomech* **42**:555–564, 2009.
19. Zainudin NA, Ramlee MH, Latip HFM, Azaman A, Seng GH, Garcia-Nieto E, Kadir MRA, Biomechanical evaluation of pin placement of external fixator in treating transverse tibia fracture: Analysis on first and second cortex of cortical bone, *Mal J Fund Appl Sci* **15**:75–59, 2019.
20. Rüedi TP, Ruedi TP, Murphy WM, *AO Principles of Fracture Management*, AO Publishing, 2000.
21. Isaksson H, Wilson W, van Donkelaar CC, Huijskes R, Ito K, Comparison of biophysical stimuli for mechano-regulation of tissue differentiation during fracture healing, *J Biomech* **39**:1507–1516, 2006.
22. Donaldson FE, Pankaj P, Simpson AHR, Bone properties affect loosening of half-pin external fixators at the pin–bone interface, *Injury* **43**:1764–1770, 2012.
23. Kumar R, Sujai S, Chethan NH, Swamy S, Results of open fractures of tibia treated by external fixator as primary and definitive procedure, *Int J Orthop Sci* **3**:179–181, 2017.
24. Giannoudis P, Papakostidis C, Roberts C, A review of the management of open fractures of the tibia and femur, *J Bone Joint Surg Br* **88**:281–289, 2006.
25. Garg P, Sodha R, Hamid FB, Somashekarappa T, Clinical study of functional outcome of external fixator device as a primary definitive treatment of open tibia fracture, *Med Legal Update* **21**:768–771, 2021.
26. Ochman S, Doht S, Paletta J, Langer M, Raschke MJ, Meffert RH, Comparison between locking and non-locking plates for fixation of metacarpal fractures in an animal model, *J Hand Surg Am* **35**:597–603, 2010.
27. Bonner T, Green S, McMurty I, A biomechanical comparison of different screw configurations in distal tibial locking plates, *Orthop Proc* **94**:20–20, 2012.
28. Weaver MJ, Chaus GW, Masoudi A, Momenzadeh K, Mohamadi A, Rodriguez EK, Vrahas MS, Nazarian A, The effect of surgeon-controlled variables on construct stiffness in lateral locked plating of distal femoral fractures, *BMC Musculoskel Dis* **22**:1–9, 2021.
29. Beingessner D, Moon E, Barei D, Morshed S, Biomechanical analysis of the less invasive stabilization system for mechanically unstable fractures of the distal femur: Comparison of titanium versus stainless steel and bicortical versus unicortical fixation, *J Trauma Acute Care Surg* **71**:620–624, 2011.
30. Mohandes Y, Tahani M, Rouhi G, Tahami M, A mechanobiological approach to find the optimal thickness for the locking compression plate: Finite element investigations, *Proc Inst Mech Eng H* **235**:408–418, 2021.
31. Ghimire S, Miramini S, Richardson M, Mendis P, Zhang L, Role of dynamic loading on early stage of bone fracture healing, *Ann Biomed Eng* **46**:1768–1784, 2018.
32. Carter DR, Beaupré GS, Giori NJ, Helms JA, Mechanobiology of skeletal regeneration, *Clin Orthop Relat Res* **355**:S41–S55, 1998.
33. Bottlang M, Lesser M, Koerber J, Doornink J, von Rechenberg B, Augat P, Fitzpatrick DC, Madey SM, Marsh JL, Far cortical locking can improve healing of fractures stabilized with locking plates, *J Bone Joint Surg Am* **92**:1652, 2010.

34. Huiskes R, Chao E, Crippen T, Parametric analyses of pin-bone stresses in external fracture fixation devices, *J Orthop Res* **3**:341–349, 1985.
35. Wu J-J, Shyr H, Chao E, Kelly P, Comparison of osteotomy healing under external fixation devices with different stiffness characteristics, *J Bone Joint Surg Am* **66**: 1258–1264, 1984.
36. Rügsegger P, Durand E, Dambacher M, Localization of regional forearm bone loss from high resolution computed tomographic images, *Osteoporosis Int* **1**:76–80, 1991.
37. Nourisa J, Rouhi G, Prediction of the trend of bone fracture healing based on the results of the early stages simulations: a finite element study, *J Mech Med Biol* **19**:1950021, 2019.